SYNTHESIS AND ELECTROCHEMICAL PROPERTIES OF POROUS CNTs-FERRITE HYBRID NANOSTRUCTURES FOR SUPERCAPACITOR[#]

Le T. T. Tam[1], Nguyen V. Hung[2], Doan T. Tung[1, 3], Ngo T. Dung[3], Hoang T. Dung[3], Nguyen T. Dung[3], Phan N. Minh[1], Phan N. Hong[4, *], Le T. Lu[1, 3, *]

[1]*Graduate University of Science and Technology, Vietnam Academy of Science and Technology, 18 Hoang Quoc Viet, Cau Giay, Ha Noi*

[2]*University of Science and Technology of Hanoi, 18 Hoang Quoc Viet, Cau Giay, Ha Noi*
[3]*Institute for Tropical Technology, Vietnam Academy of Science and Technology, 18 Hoang Quoc Viet, Cau Giay, Ha No*

[4]*Center for high technology development, Vietnam Academy of Science and Technology, 18 Hoang Quoc Viet, Cau Giay, Ha No*

[*]Email: *ltlu@itt.vast.vn*

Abstract. Carbon nanotubes (CNTs) and ferrites nanoparticles (NPs) have attracted extensive research interest owing to their potential applications in energy conversion and storage devices. In this work, ferrite NPs are prepared by solvothermal method. The NPs' surface is then modified with nitrosonium tetraflouroborate ($NOBF_4$) enabling to interact electrostatically with the COOH functionalised CNTs in phenol to form printing ink solution. The suspension is covered on ITO substrate by 3D printing method followed by cooling down to around 2 $^{\circ}$C to form porous (3D) CNTs-ferrites hybrid electrodes. The surface property of ferrite NPs and CNTs was investigated by zeta potential and FTIR measurements. The specific capacitance of the obtained CNTs-ferrite NPs hybrid material was calculated to be 10 F/g from CV measurement.

Keywords: electrode, porous, hybrid nanomaterials, supercapacitor.

Classification numbers: 2.4.2; 2.8.2; 2.10.2.

1. INTRODUCTION

Recently, energy storage and conversion devices (batteries, fuel cells, and supercapacitors) have been widely studied and used in various technology applications (computers, portable electronic devices, household and industrial electrical storage systems and electrical transportation vehicles). Among these devices, supercapacitors (SCs) are attracting special

---

[#] Presented at the Conference: "3rd Inter Workshop CPM2018"

attention of researchers in the world because of its superior properties such as longer life cycles, faster charge/discharge capability and higher power density than conventional batteries [1,2]. According to the energy storing principles, supercapacitors can be divided into two types including electric double layer capacitors (EDLCs) and pseudocapacitors (PCs) [3-5]. SCs can be considered as an intermediate storage model between battery (low power / high energy) and capacitor (high power / low energy). However, in order to widely apply the SCs in the practical use, it is required to develop high energy density SCs that can reach the current batteries, while still remain their advanced properties.

In order to increase energy density of SCs, the most popular method is increasing capacitance of electrode materials. Up to now, carbon based materials (activated carbon, CNTs and graphene) have been most widely studied and used as electrode materials for EDLCs because of its large surface area, chemical stability and high conductivity, whereas the oxide, ferrite or hydroxide materials of transition metals such as Ru, Co, Mn, Ni or conducting polymers are also extensively studied to fabricate electrodes for SCs thanks to their high charge capacitance and rapid surface redox reactions [6-11]. These materials have main drawback of low conductivity (for oxides, ferrites, hydroxides), chemically unstable (for conductive polymers) or the easy re-stack (for graphene). Therefore, in attempt to improve the disadvantages of the above materials, researches about hybrid materials based on the combination of carbon based materials (CNTs, graphene) and metal oxides to improve the performance of SCs are one of the new trends nowadays [12-17]. In our previous work, we reported on the development of a 3D printer and used it for the preparation of CNTs-ferrite NPs hybrid supercapacitor electrodes [18]. However, surface properties of the individual, such as surface charge or functional group have yet to be investigated.

In the current study, we present our results on the preparation of porous CNTs-ferrite hybrid materials as electrodes for supercapacitors by using room-temperature freeze gelation method (RTFG). The materials were investigated by various techniques, including FTIR, zeta potential, BET and Cyclic voltammetry (CV) measurements.

2. MATERIALS AND METHODS

2.1. Chemicals

Cobalt (II) acetylacetonate 99.9 % (Co(acac)$_2$), iron (III) acetylacetonate 99.9 % (Fe(acac)$_3$), oleic acid (OA) technical grade, oleylamine (OLA) 70 %, octadecanol (OCD-ol), octadecene, polyvinyl alcohol (PVA), nitrosonium tetraflouroborate (NOBF$_4$), phenol, hexane, ethanol, chloroform, dimethylformamide (DMF), tetraethylammonium tetrafluoroborate (TEABF$_4$) were ordered from Sigma-Aldrich-Singapore. Acetonitrile was received from Xilong Scientific - China. All the chemicals were used as received without further purification.

2.2. Electrode fabrication

2.2.1. Synthesis of cobalt ferrite NPs

In a typical synthesis, Co(acac)$_2$ (2.16 g, 8.4 mmol) and Fe(acac)$_3$ (6.0 g, 16.9 mmol) OCD-ol (10.8 g, 40 mmol) were added into a 100 mL three necked round bottom flask in the presence of a mixture of equimolar OA and OLA at a total concentration of 420 mM (8.4 mL, for each). The volume of octadecene solvent used was 40 mL. The reaction mixture was degassed at room

temperature for at least 30 min and then heated to 100 ^{o}C and kept at this temperature for another 30 min before increasing the temperature to 295 ^{o}C (heating rate of 5-7 ^{o}C.min^{-1}) under continuous nitrogen flow. As-synthesized NPs were purified by precipitation with the addition of ethanol, and the precipitated NPs were re-dispersed in hexane to form stable colloidal dispersions with concentrations of 1-10 mg/mL. Then the surfactant in the surface of NPs was replaced by nitrosonium tetrafluoroborate by ligand exchange reaction [18].

2.2.2. Functionalization of CNTs

CNTs (synthesized using chemical vapor deposition by Laboratory of Carbon Nanomaterials) [19] were functionalized with COOH group. Typically, 100 mg of CNTs was added in 200 ml mixture of HNO_3 and H_2SO_4 in volume ratio of 1:3. The suspension was stirred at 70 ^{o}C, 500 rpm for 5 h by a magnetic stirrer. CNTs-COOH in powder, which was obtained by filtration using 200 nm pore polytetrafluoroethylene (PTFE) membrane, was then dispersed in distilled water for mixing with NPs later.

2.2.3. Fabrication of the porous CNT/ NPs hybrid nanostructure

The CNTs – CoFe$_2$O$_4$ NPs aerogel was fabricated using freeze gelation method [20]. In a typical synthesis, 38 mg powder mixture of CNTs-COOH and CoFe$_2$O$_4$ NPs with m_{NPs}/m_{CNTs} = 2 % or 4 % and 2 mg of poly (vinyl alcohol) (PVA) were mixed in 2 mL of phenol in liquid form at 60 ^{o}C for 30 minutes. The suspension was covered on ITO substrate by 3D printing method to form an electrode which was then cooled down to around 2 ^{o}C to solidify the solution. The electrode was then taken out and stored at room condition. Aerogel film on ITO substrate was obtained after the sublimation process of phenol was completed. Aerogel made from mixture of CoFe$_2$O$_4$ NPs and CNTs with weight ratio of 2 % and 4 % are called CNTCF2 and CNTCF4, respectively.

2.3. Measurement tools

Fourier transform infrared spectrum (FTIR) of CNTs-COOH was performed using Nicolet iS50 FTIR, Thermo Scientific. The zeta potential of CNTs-COOH and CoFe$_2$O$_4$ NPs in water was recorded using Zetasizer (Malvern) [21].

A S-4800 SEM system was used to investigate the surface morphology and BET was used to determine special surface of the porous CNTs-NPs hybrid.

Electrochemical impedance spectroscopy (EIS) was performed to study the electrode at a frequency ranging from 10 mHz to 1 GHz, with a potential amplitude of 10 mV, using a standard three – electrode cell. The counter electrode was a platinum foil and the reference electrode was standard silver - silver chloride electrode in saturated KCl.

The electrolyte was composed of 0.1 M tetraethylammonium tetrafluoroborate (TEABF$_4$) in acetonitrile (Xilong Scientific). Cyclic voltammetry (CV) was conducted to investigate the electrochemical properties of the as – prepared electrodes. The potential range of CV test is set at -0.5 V to 1 V at different scan rates.

3. RESULTS AND DISCUSSION

3.1. Material characterization

A schematic of the preparation of CNTs-ferrite aerogel electrode for SCs is illustrated in Fig. 1. SEM images of the individuals and CNTs-ferrite hybrid electrode are shown in Fig. 2. Fig. 2a and b are the SEM images of CNTs-COOH and $CoFe_2O_4$ NPs. It can be seen that CNTs-COOH have long tube shape with good conductivity, which was concluded from clear image while $CoFe_2O_4$ NPs have sphere shape with the diameter of about 10 nm. SEM images of CNTs-ferrite hybrid material obtained at different magnification (Fig. 2c,d) indicate that several micro-size holes were created. This can be explained by the fact that the random dispersion of the solute during the solidification of the phenol as the solvent leads to the distribution of solvent rich regions and CNTs-ferrite rich regions.
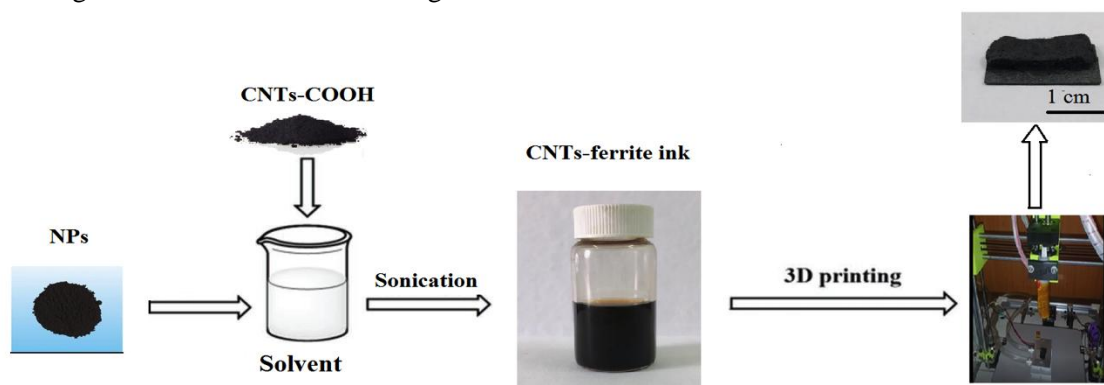
Figure 1. Schematic of the RTFG process.
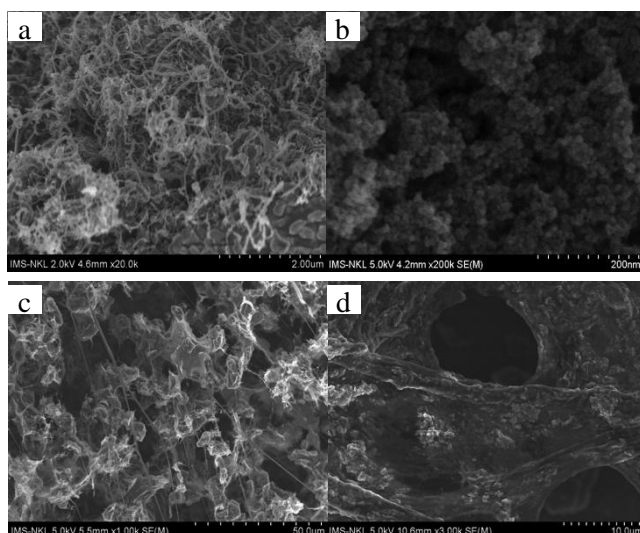
Figure 2. SEM images of CNTs-COOH (a); $CoFe_2O_4$ (b) porous CNTs-ferrite hybrid structures (c,d).
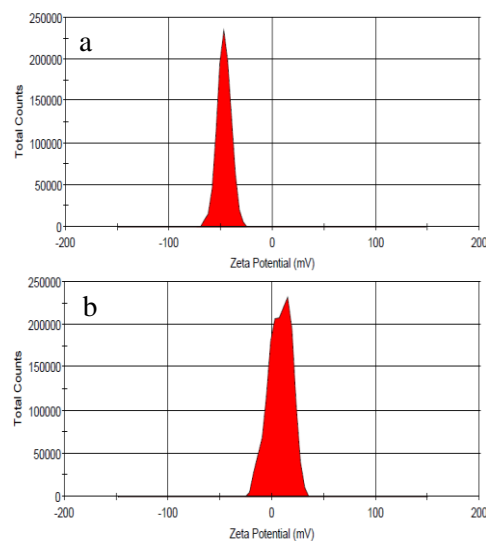
Figure 3. Zeta potential of CNTs-COOH (a) and $NOBF_4$ modified $CoFe_2O_4$ NPs (b).

Thus, when the phenol is sublimated, it leaves relatively large voids surrounding CNTs-ferrite that form porous microstructural holes and CNTs-ferrite walls. It is envident that the choice of solvent affects the microporous structure forming during initial solidification.

BET measurement was used to determine the mean specific surface area of the porous CNTs-NPs. The results show that CNTs-NPs samples have specific surface areas of approximately 114 and 85 $m^2.g^{-1}$ corresponding to CNTCF2 and CNTCF4. These low surface

area values can be explained by poor dispersion of CNTs-COOH and ferrite NPs in phenol leading to their aggregation.

In the current study, the conjugation between CNTs-COOH and NPs was conducted via electrostatic interaction. CNTs-COOH having negative charge (Fig. 3a) are attracted by positively charged $CoFe_2O_4$ NPs (Fig. 3b). The obtained zeta potentials of CNTs-COOH and $CoFe_2O_4$ NPs dispersion in water were -46.8 mV and 7.7 mV, respectively (Fig 3). These values agree with the fact that the CNTs-COOH are colloidal stable in water for months, whilst $CoFe_2O_4$ NPs are aggregated after few hours. This can be explained by the weak interactions between BF_4^- groups on the surface of $CoFe_2O_4$ NPs.
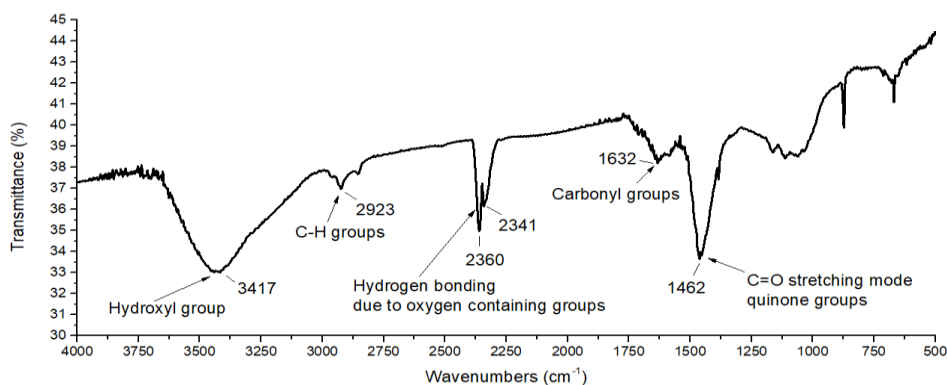
Figure 4. FTIR spectrum of CNTs-COOH.

The functionalized CNTs were characterized using FTIR to analyze functional group on CNTs wall. As shown in figure 3, CNTs was functionalized COOH group successfully. The wide peak at 3417 cm-1, the peak at 1632 cm^{-1} and the sharp peak at 1462 cm^{-1} indicate hydroxyl group, carbonyl groups and C=O of quinone groups, respectively [22]. In addition, the peak 2923 cm^{-1} and the couple peak at 2360 and 2341 cm^{-1} come from C-H groups and hydrogen bonding from oxygen containing groups, respectively [22].

3.2. Electrochemical measurements

As can be seen in Fig. 5, ITO substrate itself had a reduction peak at -0.21 V vs Ag/AgCl in saturated KCl. However, when coating a layer of PVA on ITO, the current was almost zero from -0.5V to 1.5V vs Ag/AgCl due to the electrical non-conductivity of the PVA film on the surface of ITO.

To study on the electrochemical property of the CNTs-$CoFe_2O_4$ hybrid electrode, EIS was conducted in a three-electrode mode at the frequency range of 10 mHz to 1 GHz. Fig. 6 shows the Nyquist impedance plots of CNTCF2 and CNTCF4 with the equivalent circuit of the ac impedance is inserted, respectively. The nearly straight line coming from the restricted diffusion of ions in electrolyte can be observed at low frequency. The high–frequency semicircle is explained by the model of a resistor in parallel with a capacitor with the overall contact impedance generated from the electrical connection between CNT-$CoFe_2O_4$, and the charge transfer at the contact interface between the electrode and the electrolyte. From Fig. 6, it can be seen that both the CNTCF2 and CNTCF4 have the large diameter of semicircle, which is related to the interfacial electron transfer resistance (R_{ct}). As $CoFe_2O_4$ is poor electrical conductivity, a higher mass of $CoFe_2O_4$ causes the larger electronic resistance of CNTCF4 compared to

CNTCF2 electrode. This is in accordance to the EIS analysis. The CNTCF2 exhibits a smaller R_{ct} of 119 Ω, indicating the optimal composition of CNT and $CoFe_2O_4$ NPs that lowers the inter – granular electronic resistance between electrode and the current collector.
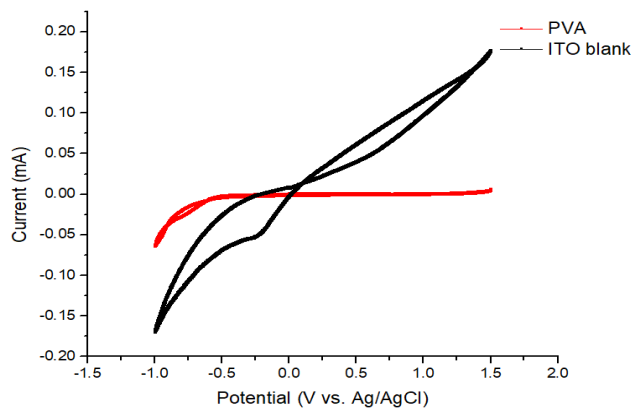
Figure 5. CV curves of PVA and ITO blank substrate.
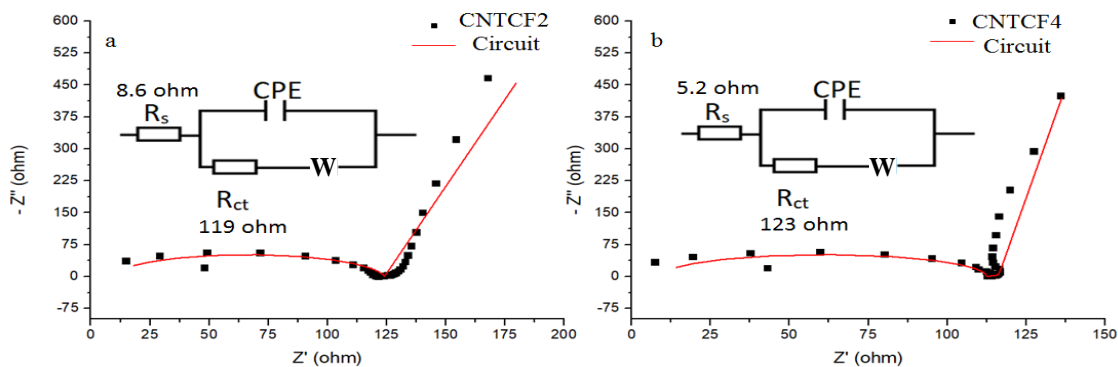
Figure 6. Nyquist impedance plots of CNTCF2 (a) and CNTCF4 (b).
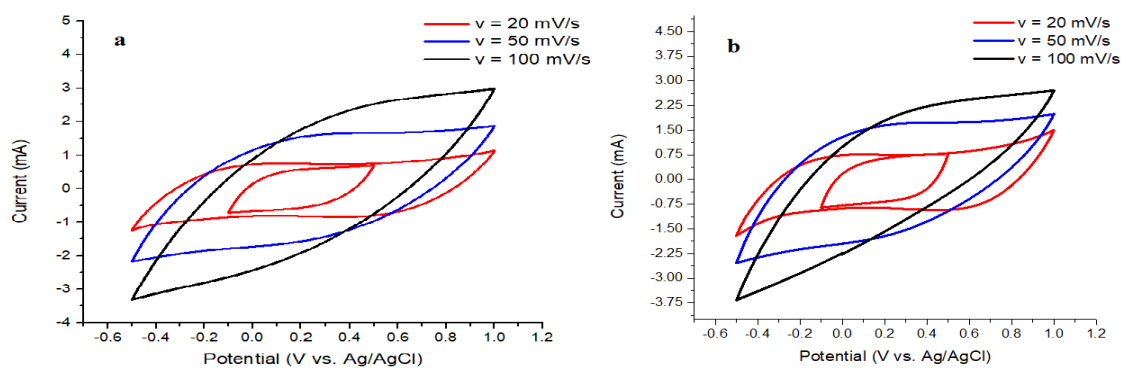
Figure 7. CV curves at different scan rates of CNTCF2 (a) and CNTCF4 (b).

In order to determine the effect of $CoFe_2O_4$ NPs in the composite aerogel CNTCF2, two potential windows were considered at the scan rate 20 mV/s, as shown in Fig. 7. From -0.1 V to

0.5 V, energy is stored only by EDL effect and from -0.5 V to 1 V, beside EDL, energy is stored by redox reaction of $CoFe_2O_4$ NPs. Although in both cases, the CV curve shapes are rectangular, positive and negative current intensity are nearly equal, the contribution of $CoFe_2O_4$ NPs can be determined by calculating specific capacitance in different potential windows. The specific capacitance (C_{sp}) can be calculated by the formula:

$$C = \frac{S}{2 \times m \times v \times \Delta V}$$

where S is the area of the CV curve, m is the mass of the active material in working electrode, v is the scan rate and ΔV is the working potential window [23-26].

From Fig. 7a, the specific capacitance of CNTCF2 at scan rate 20 mV/s in the potential range from -0.1 V to 0.5 V and from -0.5 V to 1 V are 6.8 F/g and 10.0 F/g, respectively. The higher capacitance in wider potential range is due to the redox reaction of $CoFe_2O_4$ NPs which has a reduction peak at -0.47 V at scan rate 20 mV/s. In higher scan rate, the shape of CV curve changed to mango-shape and the specific capacitance reduced to 6. F/g and 3.8 F/g at scan rate 50 mV/s and 100 mV/s, respectively.

The increase of the amount of $CoFe_2O_4$ NPs in the composite aerogel was expected to rise the specific capacitance, however, the results were opposite. As demonstrated in Figure 7b, at the scan rate of 20 mV/s, in the potential range that only EDL effect contributes to the capacitance, the specific capacitance of CNTCF4 was 7.2 F/g, which is approximate 6.8 F/g - the specific capacitance of CNTCF2 in the same potential range. In addition, in the potential range from -0.5 V to 1 V, where the capacitance value was also impacted by the presence of $CoFe_2O_4$ NPs, the specific capacitance of CNTCF4 was 9.8 F/g, which is again approximate 10.0 F/g – the specific capacitance of CNTCF2. The specific capacitance of CNTCF4 at scan rate 50 mV/s and 100 mV/s were 7.0 F/g and 3.6 F/g which are nearly equal to that of CNTCF2.

From the electrochemical behavior of CNTCF2 and CNTCF4, we can conclude that the performance of CNTCF4 is lower than that of CNTCF2, however, further optimization about the amount of NPs inside composite need to be investigated. Although it is hard to compare the quality of electrode active material considering only its specific capacitance which is affected by several parameters including current collector, electrolyte, experiment design and sample preparation technique, the CNTCF2 and CNTCF4 specific capacitance (approximately 10.0 F/g) are still low. In order to increase the specific capacitance, the interaction between CNTs and NPs needs to be improved.

4. CONCLUSIONS

In conclusion, CNTs – $CoFe_2O_4$ NPs composite aerogel film for supercapacitor electrode has been fabricated successfully using a facile method. The fabricated aerogel has 3D structure with high porosity which provides pathway for ion to diffuse and improves electrochemical performance. The initial result on the specific capacitance of the obtained CNTs-$CoFe_2O_4$ NPs hybrid material was 10.0 F/g and showed a potential to have high stability. The interaction between CNTs and NPs needs to be improved to obtain higher performance electrode. Thus, the electrostatic force requires further investigation.

REFERENCES

1. Simon P. and Gogotsi Y. – Materials for electrochemical capacitors, Y. Nat. Mater. **7** (2008) 845-854.

2. Chen J., Xia N., Zhou T., Tan S., Jiang F., and Yuan D. - Mesoporous Carbon Spheres: Synthesis, Characterization and Supercapacitance, Int. J. Electrochem. Sci. **4** (2009) 1063-1073.

3. Hsieh C. T., Chen Y. C., Chen Y. F., Huq M. M., Chen P. Y., and Jang B. S.- Microwave synthesis of titania-coated carbon nanotube composites for electrochemical capacitors, J. Power Sources **269** (2014) 526.

4. Zhu Y., Elim H. I., Foo Y.L., Yu T., Liu Y., Ji W., Lee J. Y., Shen Z., Wee A. T. S. and Thong J. T. L. - Multiwalled Carbon Nanotubes Beaded with ZnO Nanoparticles for Ultrafast Nonlinear Optical Switching, Adv. Mater. **18** (2006) 587.

5. Du C., Yeh J., and Pan N. - High power density supercapacitors using locally aligned carbon nanotube electrodes, Nanotechnology **16** (2005) 350.

6. Peigney A., Laurent C., Flahaut E., Bacsa R. R. and Rousset A. - Specific surface area of carbon nanotubes and bundles of carbon nanotubes, Carbon **39** (2001) 507-514 .

7. Liu C., Yu Z., Neff D., Zhamu A. and Jang B. Z. - Graphene-Based Supercapacitor with an Ultrahigh Energy Density, Nano Lett. **10** (2010) 4863-4868 .

8. Zhu Y. W., Murali S., Stoller M. D., Velamakanni A., Piner R. D. and Ruoff R. S. - Microwave assisted exfoliation and reduction of graphite oxide for ultracapacitors, Carbon **48** (2010) 2118 .

9. Yu G., Xie X., Pan L., Bao Z. and Cui Y. - Hybrid nanostructured materials for high-performance electrochemical capacitors, Nano Energy **2** (2013) 213-234.

10. Zheng J. P., Cygan P. J. and Jow T. R. - Hydrous Ruthenium Oxide as an Electrode Material for Electrochemical Capacitors, J. Electr. Soc. **142** (1995) 2699-2703.

11. Yang P., Ding Y., Lin Z., Chen Z., Li Y., Qiang P., Ebrahimi M., Mai W., and Wang J. L. - Low-cost high-performance solid-state asymmetric supercapacitors based on MnO_2 nanowires and Fe_2O_3 nanotubes, Nano letter. **14** (2014) 731-736.

12. Lee S. W., Kim J., Chen S., Hammond P. T., and Shao-Horn Y. - Carbon Nanotube/Manganese Oxide Ultrathin Film Electrodes for Electrochemical Capacitors, ACS Nano **4** (2010) 3889.

13. Park J. H., Ko J. M., and Park O. O. - Carbon Nanotube/RuO_2 Nanocomposite Electrodes for Supercapacitors, J. Electrochem. Soc. **150** (2003) A864.

14. Chen P. C., Shen G., Sukcharoenchoke S., and Zhou C. - Flexible and transparent supercapacitor based on In2O3 nanowire/carbon nanotube heterogeneous films, Appl. Phys. Lett. **94** (2009) 043113.

15. Chen Z., Augustyn V., Wen J., Zhang Y., Shen M., Dunn B., and Lu Y. - High-Performance Supercapacitors Based on Intertwined CNT/V_2O_5 Nanowire Nanocomposites, Adv. Mater. **23** (2011) 791.

16. Aravinda L., Nagaraja K., Nagaraja H., Bhat K. U., and Bhat B. R. - ZnO/carbon nanotube nanocomposite for high energy density supercapacitors, Electrochim. Acta **95** (2013) 119.

17. Lin P., She Q., Hong B., Liu X., Shi Y., Shi Z., Zheng M., and Dong Q. - The Nickel Oxide/CNT Composites with High Capacitance for Supercapacitor, J. Electrochem. Soc. **157** (2010) A818.

18. Dung H. T., Dung N. T., Dung T. Q., Dung D. T., Yen N. T., Tam L. T. T., Thu T. V., Hong P. N. and Lu L. T. - Fabrication and Characterisation of Supercapacitor Electrode by 3D printing, Vietnam Journal of Science and Technology **56**(5) (2018) 574-581.

19. Van Chuc N., Dung N. D., Hong P. N., Quang L. D., Khoi, P. H., & Minh, P. N.- Synthesis of Carbon Nanotubes on Steel Foils, J. Korean Physic. Soc. **52**(5) (2008) 1368.

20. Lin Y., Liu F., Casano G., Bhavsar R., Kinloch I. A. and Derby B. - Pristine Graphene Aerogels by Room-Temperature Freeze Gelation, Adv. Mater. **28**(36) (2016) 7993-8000.

21. Tantra R., Schulze P. and Quincey P. - Effect of nanoparticle concentration on Zeta-potential measurement results and reproducibility, Particuology **8**(3) (2010) 279–285.

22. Mombeshora E. T., Simoyi R., Nyamori V. O. and Ndungu P. G. - Multiwalled carbon nanotube-titania nanocomposites: Understanding nano-structural parameters and functionality in dye-sensitized solar cells, S. Afr. J. Chem. **68** (2015) 153-164.

23. Han D., Xu P., Jing X., Wang J., Yang P., Shen Q., Liu J., Song D., Gao Z., Zhang M. - Trisodium Citrate Assisted Synthesis of Hierarchical NiO Nanospheres with Improved Supercapacitor Performance, J. Power Sources **235** (2013) 45-53.

24. Lee J. W., Hall A. S., Kim J. D., Mallouk T. E. – A facile and template-free hydrothermal synthesis of Mn_3O_4 nanorods on graphene sheets for supercapacitor electrodes with long cycle stability, Chem. Mater. **24** (2012) 1158-1164.

25. Wang J.G., Yang Y., Huang Z.H., Kang F. - Rational synthesis of MnO_2/conducting polypyrrole@carbon nanofiber triaxial nano-cables for high-performance supercapacitors, J. Mater. Chem. **22** (2012) 16943-16949.

26. Lee T., Yun T., Park B., Sharma B., Song H.K., Kim B.S. - Hybrid multilayer thin film supercapacitor of graphene nanosheets with polyaniline: importance of establishing intimate electronic contact through nanoscale blending, J. Mater. Chem. **22** (2012) 21092-21099.